

Supporting Information

Mechanochemical Effect on the Electrochemical Properties of $\text{Na}_3(\text{VO})_2(\text{PO}_4)_2\text{F}$ Positive Electrode for Sodium-Ion Batteries

William G. Morais^{a*}, Eduardo C Melo, and Roberto M. Torresi*

*Departamento de Química Fundamental, Instituto de Química, Universidade de São Paulo, Av.
Prof. Lineu Prestes, 748, 05508-000, São Paulo, SP, Brazil.*

^a Present address: Center for Sustainable Energy – SE, Fondazione Bruno Kessler – FBK. Via
Sommarive 18, 38123 Povo (TN), Italy

E-mail: rtorresi@iq.usp.br (RMT), wgomesdemorais@fbk.eu (WGM).

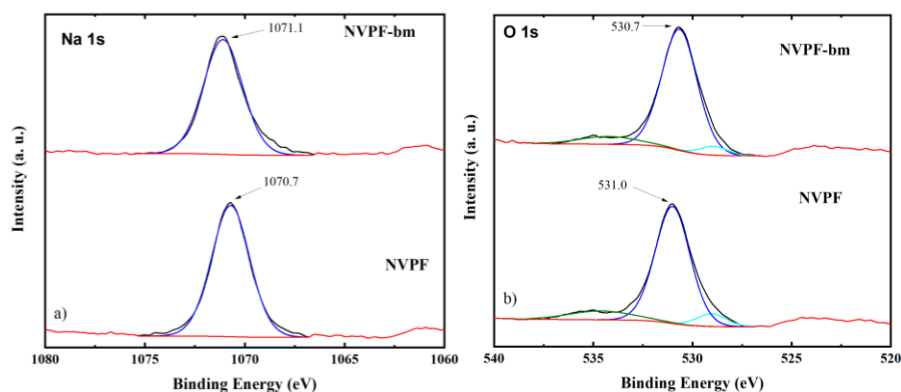
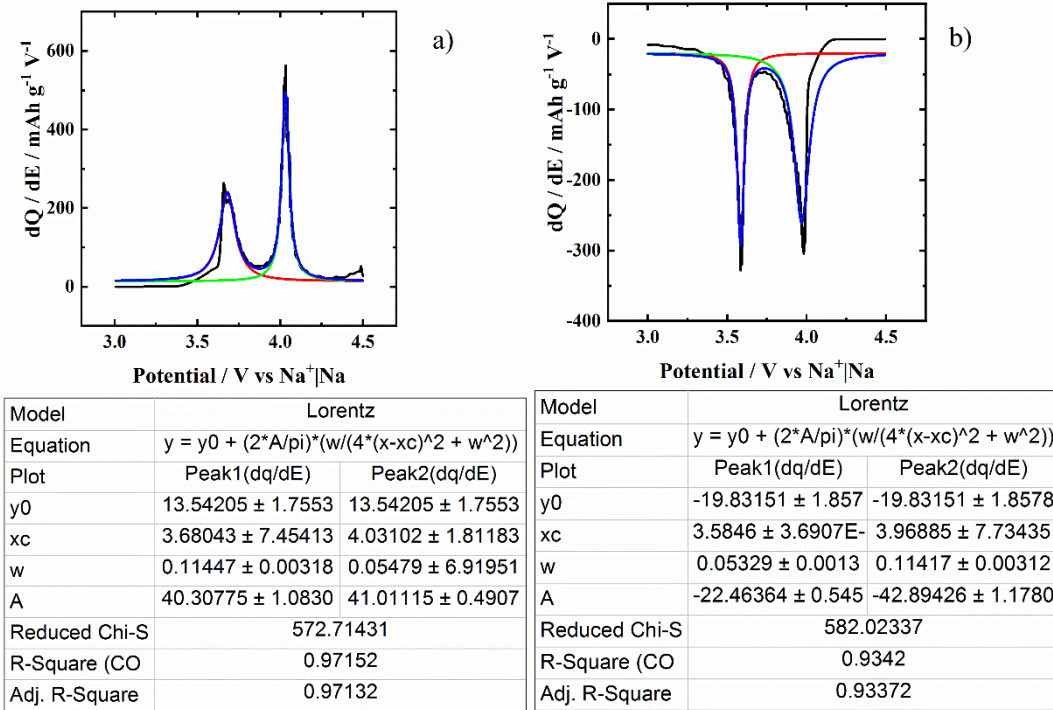
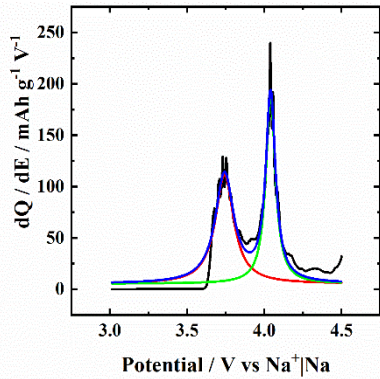


Figure S1: XPS spectra and corresponding deconvolution results of the orbital peak a) Na 1s and b) O 1s of the NVPF and NVPF-bm electrodes.

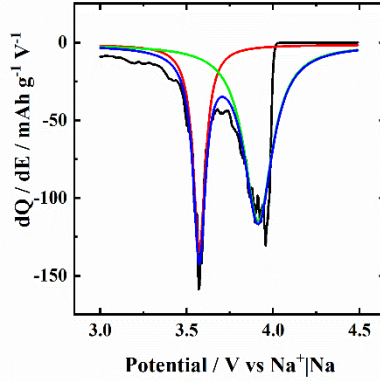
The obtained dQ/dE plots were fitted with the aid of the software Origin, version 2020, OriginLab Corporation. The area of each peak was normalized by the total area of the full charge (or discharge) curve. Figures S1 and S2 show the fitted plots for the NVPF and NVPF-bm, respectively.





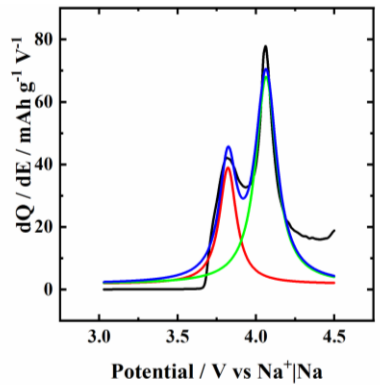
c)

Model	Lorentz	
Equation	$y = y_0 + (2 \cdot A / \pi) \cdot (w / (4 \cdot (x - x_c)^2 + w^2))$	
Plot	Peak1(dq/dE)	Peak2(dq/dE)
y0	5.38082 ± 1.2929	5.38082 ± 1.29299
xc	3.74202 ± 0.0015	$4.04052 \pm 5.20794E$
w	0.14426 ± 0.0062	0.07532 ± 0.00191
A	24.06491 ± 0.989	21.65575 ± 0.50557
Reduced Chi-S	137.24737	
R-Square (COD)	0.95936	
Adj. R-Square	0.95865	



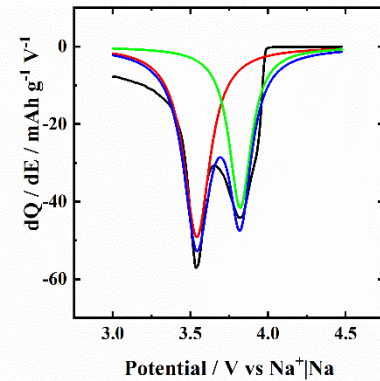
d)

Model	Lorentz	
Equation	$y = y_0 + (2 \cdot A / \pi) \cdot (w / (4 \cdot (x - x_c)^2 + w^2))$	
Plot	Peak1(dq/dE)	Peak2(dq/dE)
y0	-1.44403 ± 1.64952	-1.44403 ± 1.6495
xc	3.57307 ± 9.92905	3.91364 ± 0.00202
w	0.08521 ± 0.00363	0.19891 ± 0.00875
A	-17.71965 ± 0.6963	-35.43546 ± 1.583
Reduced Chi-S	168.89527	
R-Square (CO)	0.92057	
Adj. R-Square	0.91915	



e)

Model	Lorentz	
Equation	$y = y_0 + (2 \cdot A / \pi) \cdot (w / (4 \cdot (x - x_c)^2 + w^2))$	
Plot	Peak1(dq/dE)	Peak2(dq/dE)
y0	1.75908 ± 0.7587	1.75908 ± 0.75876
xc	3.82111 ± 0.0048	4.06461 ± 0.00292
w	0.13098 ± 0.0164	0.16334 ± 0.00983
A	7.65513 ± 0.8197	17.00534 ± 0.9435
Reduced Chi-Sqr	34.84459	
R-Square (COD)	0.92526	
Adj. R-Square	0.92216	



f)

Model	Lorentz	
Equation	$y = y_0 + (2 \cdot A / \pi) \cdot (w / (4 \cdot (x - x_c)^2 + w^2))$	
Plot	Peak1(dq/dE)	Peak2(dq/dE)
y0	-0.05956 ± 0.6526	-0.05956 ± 0.6526
xc	3.54101 ± 0.00369	3.8206 ± 0.00395
w	0.20622 ± 0.01259	0.17269 ± 0.01357
A	-15.90193 ± 0.918	-11.26327 ± 0.805
Reduced Chi-S	19.72584	
R-Square (COD)	0.93746	
Adj. R-Square	0.93486	

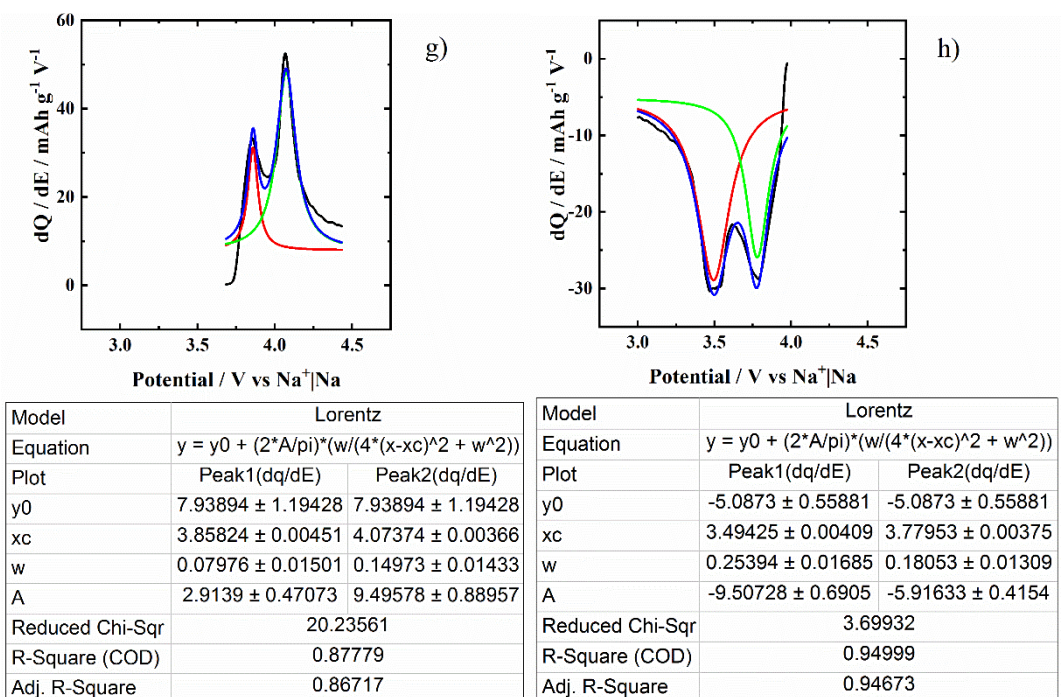
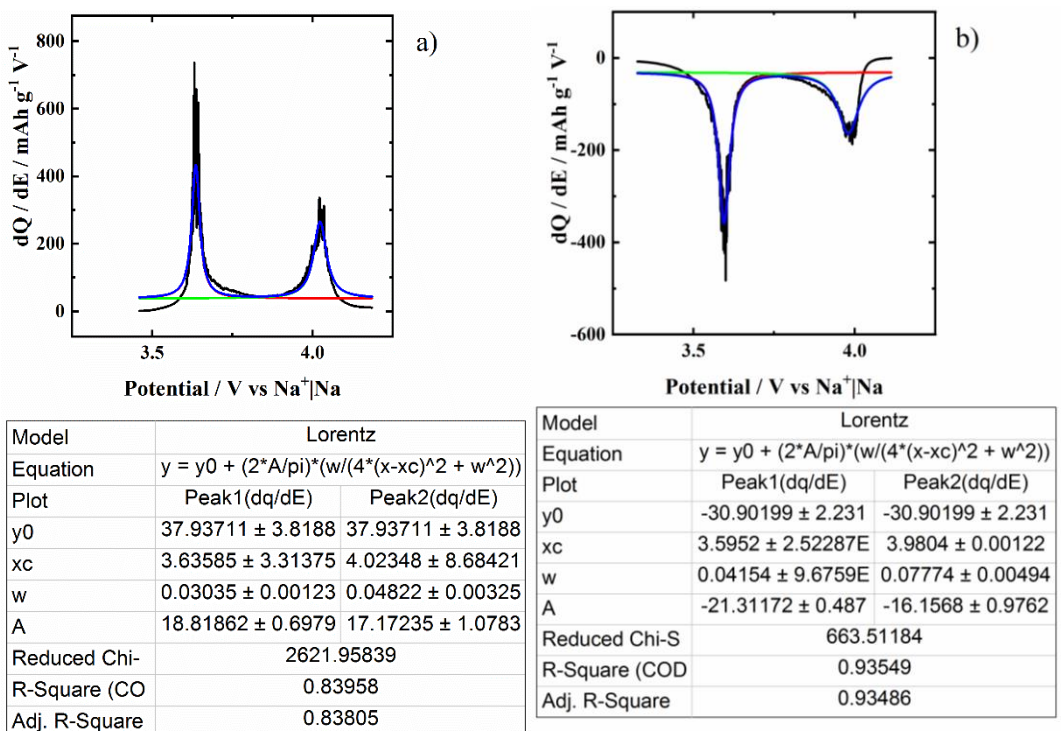
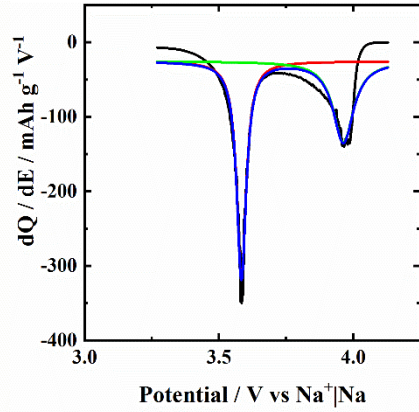
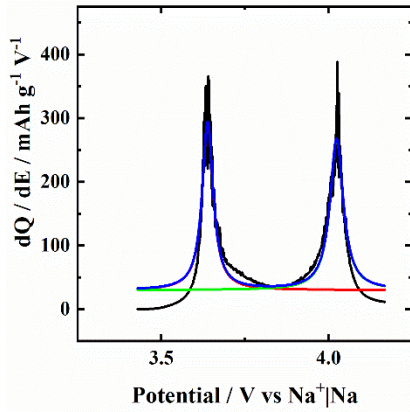


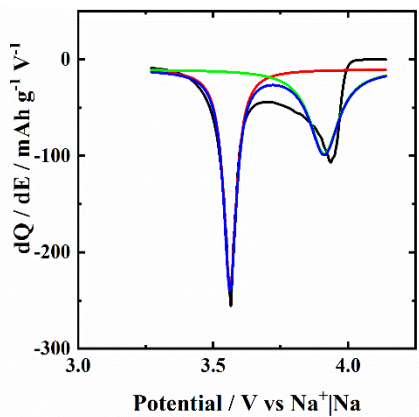
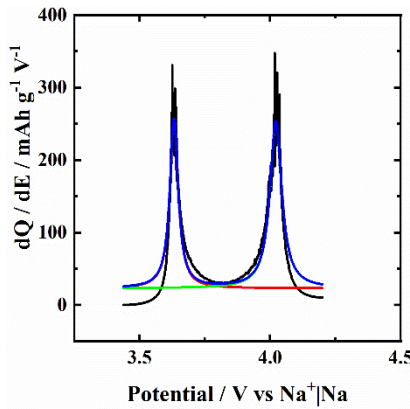
Figure S2: Fitting of the dQ/dE peaks of the NVPF electrode at (a, b) 10, (c, d) 20, (e, f) 50 and (g, h) 70 $\mu\text{A g}^{-1}$.





Model	Lorentz	
Equation	$y = y_0 + (2*A/\pi)*(w/(4*(x-xc)^2 + w^2))$	
Plot	Peak1(dq/dE)	Peak2(dq/dE)
y0	30.08333 ± 2.2481	30.08333 ± 2.2481
xc	3.63873 ± 3.39761	4.02455 ± 4.37333
w	0.03942 ± 0.00132	0.0481 ± 0.00168
A	16.31804 ± 0.5076	17.87592 ± 0.5967
Reduced Chi-	713.203	
R-Square (CO	0.91629	
Adj. R-Square	0.91541	

Model	Lorentz	
Equation	$y = y_0 + (2*A/\pi)*(w/(4*(x-xc)^2 + w^2))$	
Plot	Peak1(dq/dE)	Peak2(dq/dE)
y0	-25.57376 ± 2.0402	-25.57376 ± 2.040
xc	3.58368 ± 2.66315	3.96322 ± 0.0016
w	0.04275 ± 0.00103	0.09227 ± 0.0064
A	-19.60521 ± 0.4577	-15.78914 ± 1.057
Reduced Chi-S	270.89365	
R-Square (CO	0.96657	
Adj. R-Square	0.9659	



Model	Lorentz	
Equation	$y = y_0 + (2*A/\pi)*(w/(4*(x-xc)^2 + w^2))$	
Plot	Peak1(dq/dE)	Peak2(dq/dE)
y0	22.91637 ± 2.1776	22.91637 ± 2.1776
xc	3.63202 ± 3.62022	4.02206 ± 4.41271
w	0.03872 ± 0.00141	0.05443 ± 0.00175
A	14.20209 ± 0.4816	19.68405 ± 0.6243
Reduced Chi-	566.8149	
R-Square (CO	0.92274	
Adj. R-Square	0.92184	

Model	Lorentz	
Equation	$y = y_0 + (2*A/\pi)*(w/(4*(x-xc)^2 + w^2))$	
Plot	Peak1(dq/dE)	Peak2(dq/dE)
y0	-10.07979 ± 2.9127	-10.07979 ± 2.912
xc	3.56251 ± 6.32714	3.91167 ± 0.0036
w	0.05736 ± 0.00243	0.13111 ± 0.0145
A	-20.4024 ± 0.83285	-18.02952 ± 1.985
Reduced Chi-S	202.77533	
R-Square (CO	0.95911	
Adj. R-Square	0.95715	

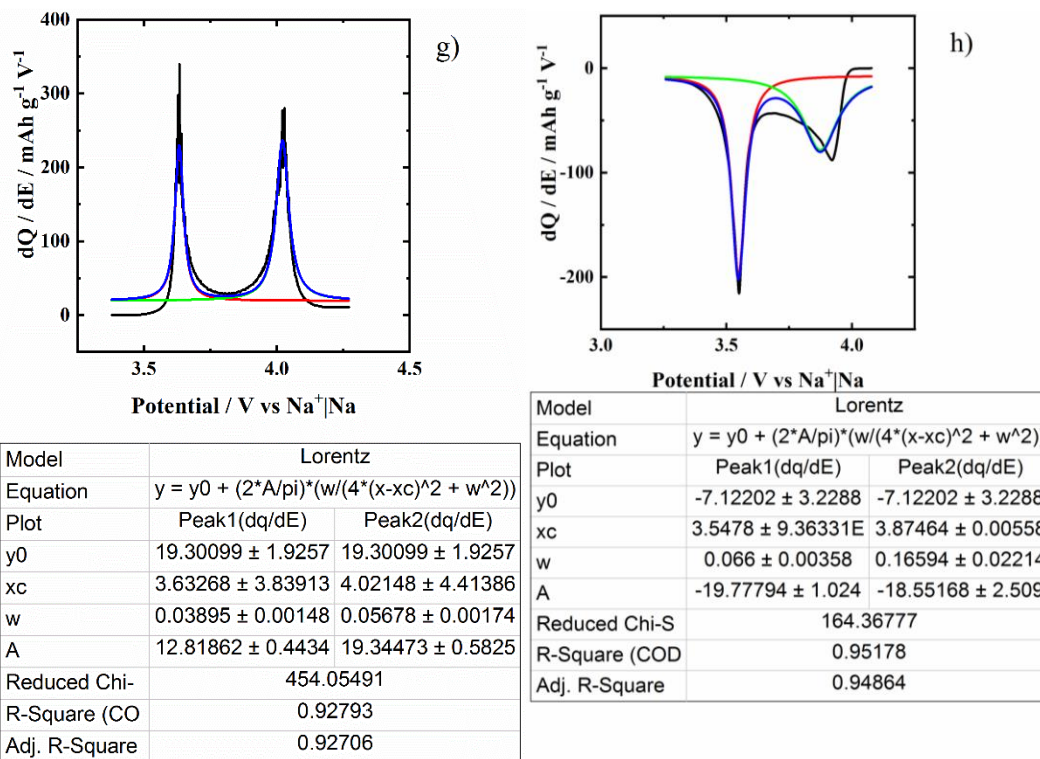
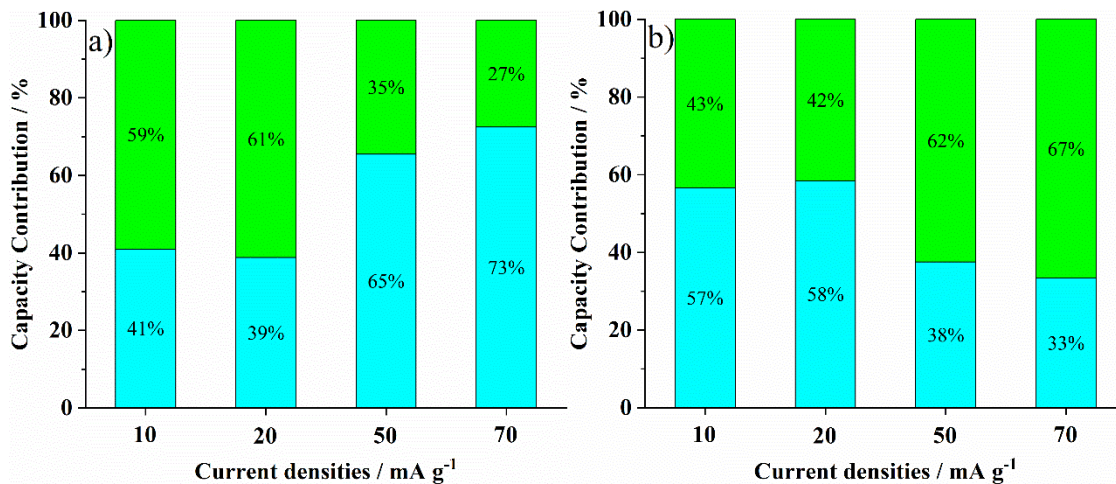


Figure S3: Fitting of the dQ/dE peaks of the NVPF-bm electrode at (a, b) 10, (c, d) 20, (e, f) 50 and (g, h) 70 $\mu\text{A g}^{-1}$.



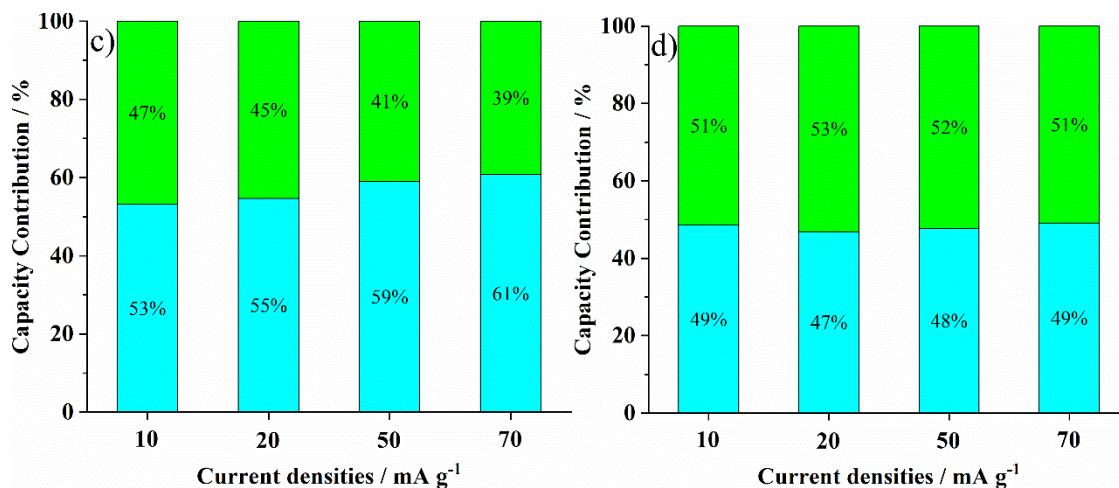


Figure S4: Capacity contributions from the (a, b) Na_1^+ and (c, d) Na_2^+ for the (light green) charge and (light blue) discharge processes of the (a, b) NVPF and (c, d) NVPF-bm electrodes.

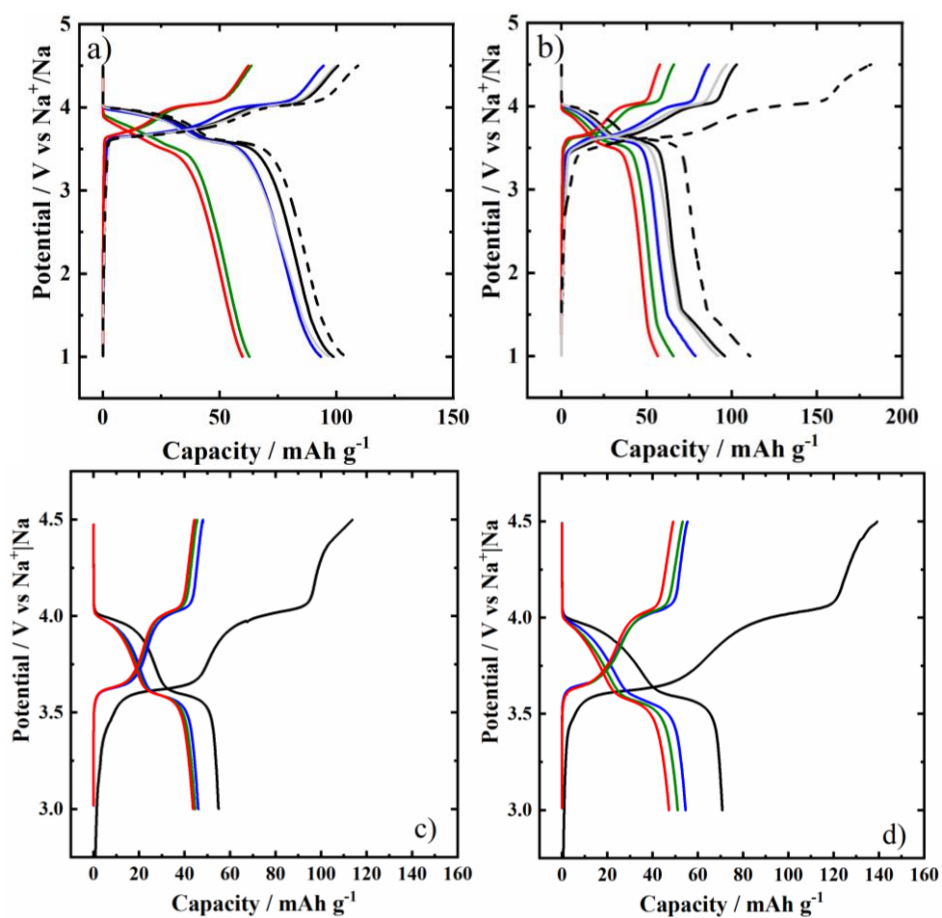


Figure S5: Charge and discharge curves NVPF (a) and NVPF-bm (b) electrodes at 0.01 (—), 0.02 (—), 0.05 (—) and 0.07 (—) $A g^{-1}$, with the 1st (—) and 100th (—) cycle at 0.01 $A g^{-1}$. 1st (—), 50th (—), 100th (—) and 150th (—) cycle of charge/discharge of the NVPF (c) and NVPF-bm (d) electrodes charged at 0.01, discharged at 0.02 $A g^{-1}$.

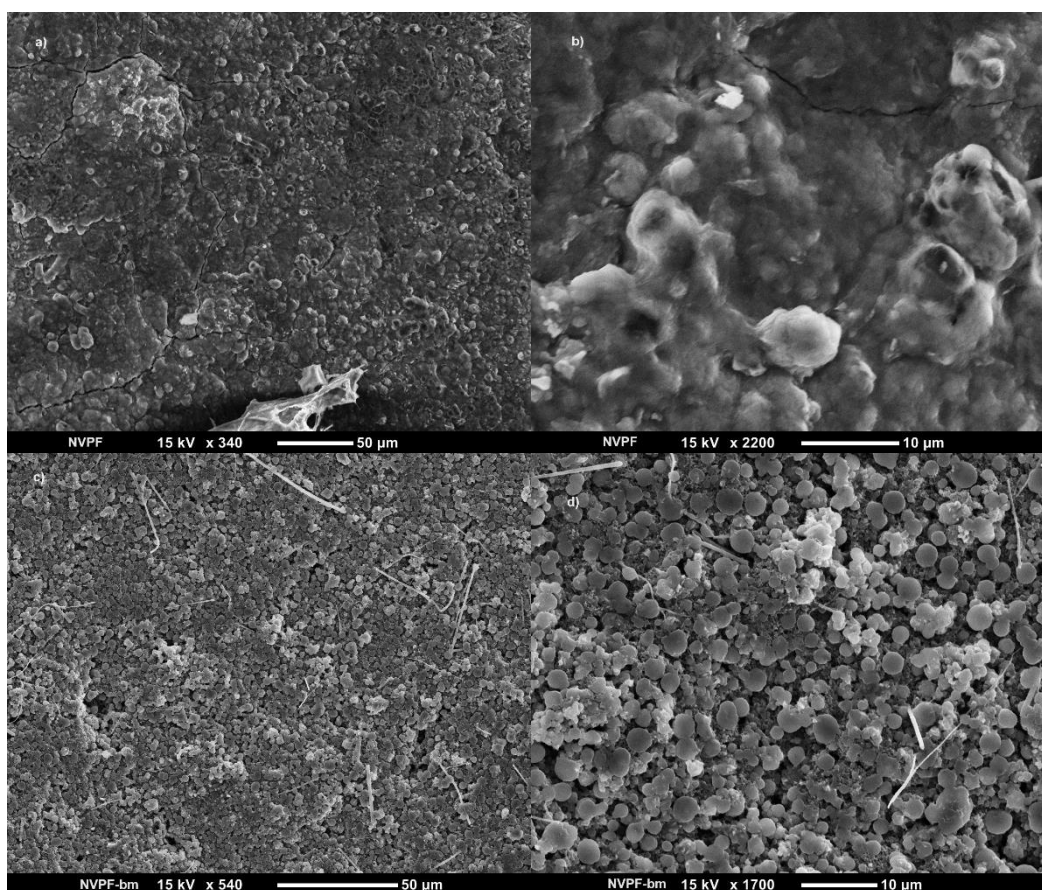


Figure S6: Post-mortem SEM images of the NVPF (a, b) and NVPF-bm (c, d) electrodes.

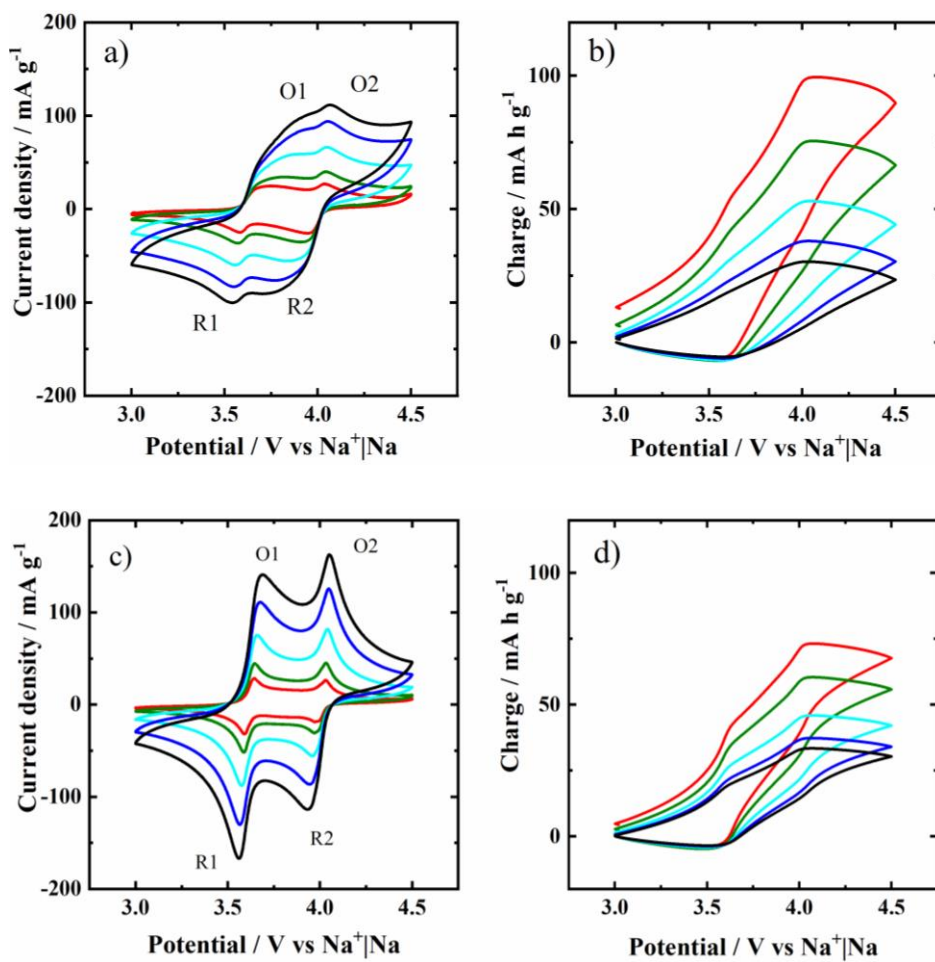


Figure S7: Cyclic voltammograms and charge variation as a function of the cell potential of the NVPF (a, b) and NVPF-bm (c, d). $v = 0.05$ (—), 0.10 (—), 0.25 (—), 0.50 (—) and 0.75 mV s⁻¹